

Record low Antarctic sea ice coverage indicates a new sea ice state

Ariaan Purich ¹✉ & Edward W. Doddridge ²

In February 2023, Antarctic sea ice set a record minimum; there have now been three record-breaking low sea ice summers in seven years. Following the summer minimum, circumpolar Antarctic sea ice coverage remained exceptionally low during the autumn and winter advance, leading to the largest negative areal extent anomalies observed over the satellite era. Here, we show the confluence of Southern Ocean subsurface warming and record minima and suggest that ocean warming has played a role in pushing Antarctic sea ice into a new low-extent state. In addition, this new state exhibits different seasonal persistence characteristics, suggesting that the underlying processes controlling Antarctic sea ice coverage may have altered.

¹School of Earth, Atmosphere and Environment, and ARC Special Research Initiative for Securing Antarctica's Environmental Future, Monash University, Clayton, Kulin Nations, Australia. ²Australian Antarctic Program Partnership, Institute for Marine and Antarctic Studies, University of Tasmania, nipaluna/Hobart, Tasmania, Australia. ✉email: ariaan.purich@monash.edu

Antarctic sea ice is a critical component of the global climate system^{1–3}. Climatologically, Antarctic sea ice reaches its annual minimum in mid-February to early March. Sea ice coverage in January and February 2023 broke monthly and daily sea ice extent records for this time of year⁴. On 10 February 2023, sea ice coverage broke the record daily minimum of 1.91 million square kilometres set one year earlier on 21 February 2022^{4,5}. On 19 February 2023, a new minimum Antarctic sea ice extent of 1.77 million square kilometres was observed⁴, 1.02 million square kilometres (36%) less than the 1979–2022 average daily minimum sea ice coverage.

In late-December 2022, sea ice extent plummeted and remained exceptionally low during January 2023 (Fig. 1a). Antarctic sea ice coverage was 1.74 million square kilometres less than the average over 1979–2022 for January, representing the then second largest monthly-mean anomaly in sea ice coverage over the satellite record, after December 2016 (2.01 million square

kilometres less than the 1979–2022 December average; Fig. 1a). The exceptionally low sea ice continued in February, with monthly-mean coverage 1.12 million square kilometres below normal. As a percentage of the monthly climatology, sea ice extents in January and February 2023 were the largest negative anomalies recorded in the 44-year observational period (35% and 37%, respectively Fig. 1b).

Following the summer minimum, Antarctic sea ice coverage has remained at, or near, record low values during 2023 (Figs. 1a, 2). For the time of year, Antarctic sea ice coverage was the lowest on record from the beginning of the year until early March, and again throughout May and June. At the time of analysis (early July 2023), the June monthly sea ice extent anomaly of 2.33 million square kilometres less than the average over 1979–2022 for June is the most negative anomaly of the satellite record, exceeding the monthly anomalies of January 2023, and December 2016, and roughly double the size of the previous record negative anomaly in

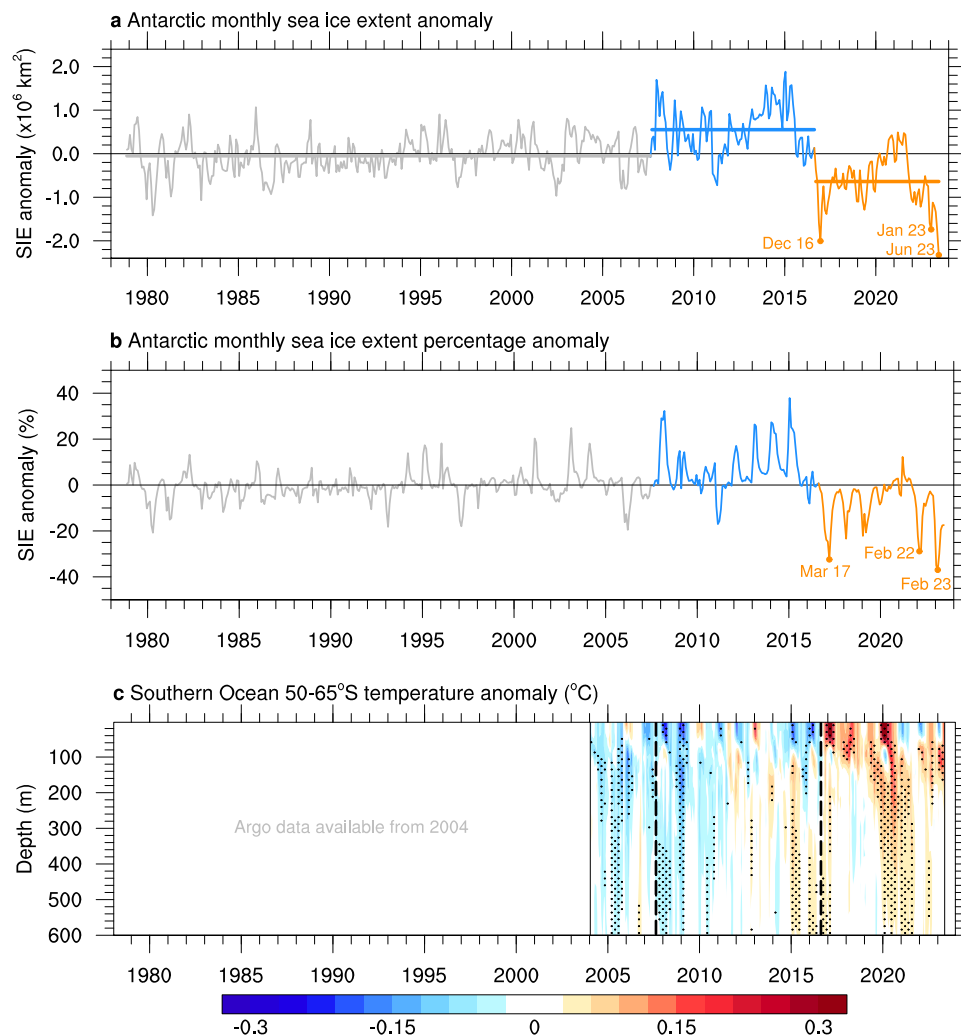


Fig. 1 Antarctic sea ice extent and Southern Ocean temperature anomalies showing the low sea ice and warm ocean state since 2016. a Antarctic monthly sea ice extent (SIE) anomaly time series from the National Snow and Ice Data Center over the satellite period, November 1978 to June 2023, in millions of square kilometres. Sea ice extent anomalies are calculated relative to the 1979–2022 climatology. Two change points are detected, separating the time series into three periods: November 1978 to August 2007 (grey), September 2007 to August 2016 (blue), and September 2016 to June 2023 (orange). The means of each period are shown by the horizontal lines and are statistically distinguishable. **b** Antarctic monthly SIE anomaly time series expressed as a percentage of the monthly climatology over 1979–2022. Periods are coloured as in (a). Record minima months occurring since 2016 are noted in (a, b). **c** Southern Ocean 50–65°S temperature anomaly time series from Argo over January 2004 to May 2023, in degrees Celsius. Ocean temperature anomalies are calculated relative to the 2004–2022 climatology. Dashed vertical lines show the sea ice extent change points. Stippling indicates values outside ± 1 standard deviation, where the standard deviation is calculated independently at each depth level to account for the change in magnitude of the variability with depth. Warm anomalies shown in orange and red are evident below 100 m from 2015, and at the surface from late 2016.

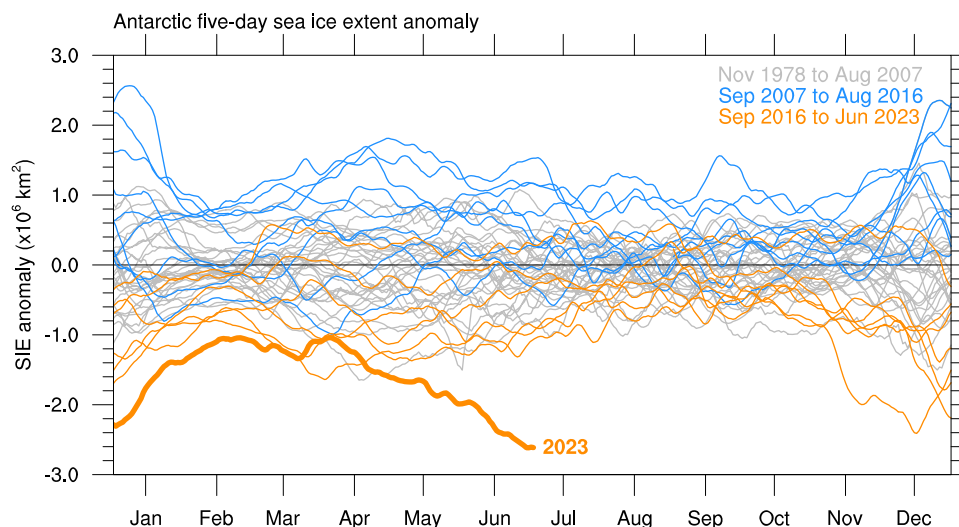


Fig. 2 Sea ice extent has remained exceptionally low throughout the first half of 2023. Antarctic five-day sea ice extent anomalies in millions of square kilometres for each year from the National Snow and Ice Data Center. Sea ice extent anomalies are calculated relative to the 1979–2022 climatology. Anomalies are coloured by period as in Fig. 1: November 1978 to August 2007 (grey), September 2007 to August 2016 (blue), and September 2016 to June 2023 (orange). January to June 2023 is shown in bold orange, with the largest negative areal extent anomaly of the satellite era observed during June 2023.

June (Fig. 2). This raises important questions on the drivers of this extremely low sea ice coverage.

Results and Discussion

A new state for Antarctic sea ice. The temporal evolution of Antarctic sea ice extent anomalies over the observational period (Fig. 1a) has conventionally been described as a gradual multi-decadal increase, followed by a precipitous decrease in 2016⁶. However, applying an algorithm for detecting change points in the sea ice extent anomaly time series (Methods) identifies two change points in the 44-year time series, separating the sea ice anomaly record into three periods with statistically distinguishable means (t-test, $p < 0.01$; Methods). The first period spans from the beginning of the record in November 1978 until August 2007; the second from September 2007 until August 2016; and the third from September 2016 until June 2023. Variability in the first period is lower than in the subsequent periods (F-test, $p < 0.01$), but variability in the two later periods is not statistically distinguishable.

These statistically significant changes in mean and variability raise the possibility that recent sea ice extremes are not just manifestations of interannual variability. The change points identified (Fig. 1a) do not align with changes in large scale climate modes known to impact sea ice variability, such as the Southern Annular Mode⁷, the El Niño Southern Oscillation, the Interdecadal Pacific Oscillation^{8,9}, or the Atlantic Multidecadal Oscillation^{10,11} (Methods, Supplementary Fig. 1). Furthermore, climate modes have strong regional impacts^{7–11}, while the current low sea ice state is characterised by circumpolar low sea ice anomalies (Fig. 3, Supplementary Fig. 2).

The multi-decade increase in Antarctic sea ice that peaked in 2014, identified here as a high sea ice state between mid-2007 and mid-2016, has been examined extensively, with contributions from high-latitude winds^{12,13} and Antarctic meltwater^{14,15} suggested to have played a role. Positive ocean-sea ice feedbacks may have perpetuated the high sea ice coverage¹⁶ during this period. In spring 2016, Antarctic sea ice rapidly transitioned to a new, low sea ice state.

The atmosphere is an important driver of Antarctic sea ice variability and change. Individual extreme sea ice events have

been linked to anomalous atmospheric circulation events. For example, the strong meridional circulation associated with zonal wave number three contributed to the low sea ice in spring 2016¹⁷, while a strong Amundsen Sea Low circulation in spring 2021 influenced the low spring/summer sea ice conditions in 2021/22^{18,19}. However, the phase of the Southern Annular Mode cannot account for the low Antarctic sea ice over recent years: the positive phase of the Southern Annular Mode has historically been associated with colder sea surface temperatures and increased sea ice extent⁷, and in line with this, the 2017 record summer sea ice minimum (Fig. 1a, b) occurred at a time of anomalously warm surface temperatures in the Southern Ocean (Fig. 1c) and an anomalously negative Southern Annular Mode²⁰. In contrast, the 2022 and 2023 record sea ice minima occurred when surface temperatures were close to the climatological mean (Fig. 1c) and the Southern Annular Mode was anomalously positive²¹, while the subsurface ocean was anomalously warm. The breakdown in this Southern Annular Mode-sea ice relationship raises the possibility that Antarctic sea ice has entered a new regime in which previously important relationships no longer dominate sea ice variability. Increased zonal asymmetry in the Southern Annular Mode over the satellite era may be important in contributing to this change²², however here we focus on an important consistency across the three recent record low sea ice summers: a warm subsurface ocean.

Southern ocean warming. The subsurface Southern Ocean is warming^{23–25} (Fig. 1c), which we suggest is linked to the current low sea ice state, and may have caused a regime shift in Antarctic sea ice²⁶. Southern Ocean warming since the mid 20th Century has been attributed primarily to increasing greenhouse gases^{27–29}, with ozone depletion playing a secondary role^{27,28}. Internally-generated variability may have also contributed to the recent accelerated Southern Ocean warming (Fig. 1c)^{30,31} but alone it cannot account for the observed warming³¹.

Using a gridded Argo dataset (Methods), we present the circumpolar average ocean temperature anomaly between 50–65°S (Fig. 1c)³⁰. The shift from cold subsurface temperatures to warm subsurface temperatures (below 100 m; Fig. 1c) occurs approximately one year before the second change point identified

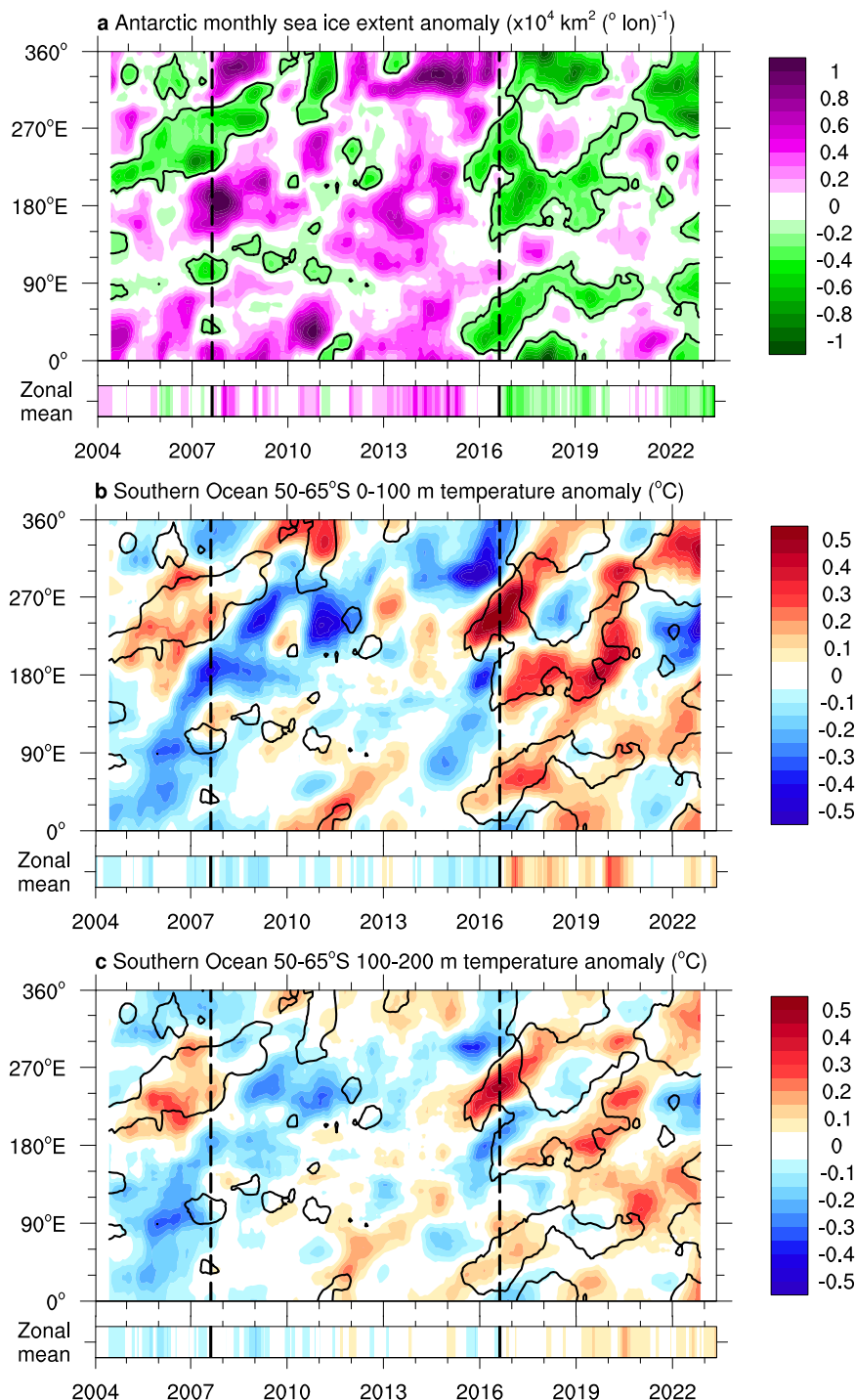


Fig. 3 Patterns of sea ice and ocean temperature anomalies show strong regional agreement in the current sea ice period, with warm subsurface ocean anomalies emerging prior to the transition to the current low sea ice state. Hovmöller diagrams of (a) longitudinal sea ice extent anomalies, (b) 0–100 m temperature anomalies, and (c) 100–200 m temperature anomalies. Sea ice extent is calculated for each longitude from gridded sea ice concentration (Methods) and anomalies are calculated relative to the 1979–2022 climatology. Ocean temperature is averaged over 50–65°S and anomalies are calculated relative to the 2004–2022 climatology. Smoothing is applied to all fields using a running average both temporally (over 12 months) and longitudinally (over 20°). Dashed vertical lines show the sea ice extent change points. Black contours in (a) indicate the $-0.2 \times 10^4 \text{ km}^2 (\text{° lon})^{-1}$ sea ice extent anomaly contour. The same black sea ice contours are overlain in (b, c) to allow comparison between sea ice anomalies and underlying ocean temperature anomalies. The unsmoothed zonal mean of each field is shown below each Hovmöller diagram.

in the sea ice extent time series (Fig. 1a), strongly suggesting that the current low sea ice extent state is due, at least partly, to subsurface ocean warming.

Examining the temporal evolution of regional Antarctic sea ice coverage and subsurface temperature (Fig. 3) reveals the

widespread nature of low sea ice coverage and warm ocean temperatures in the current low sea ice state. This can also be seen in spatial maps of Antarctic sea ice coverage and subsurface temperatures across the three identified periods (Supplementary Fig. 2). While there is evidence that climate modes contributed to

low sea ice coverage in recent individual years^{17–19,30}, when averaged over the seven years of the current period, a circumpolar decline in sea ice is seen (Fig. 3a, Supplementary Fig. 2d), coincident with a circumpolar subsurface ocean warming (Fig. 3c, Supplementary Fig. 2d). Importantly, subsurface ocean warming occurs prior to the reduction in Antarctic sea ice (Fig. 3c, Supplementary Fig. 2c), with strong spatial agreement between warm anomalies at 100–200 m depth in 2015 (340–20°E and 190–250°E), and the subsequent strong negative sea ice anomalies in 2016 (10–90°E and 190–290°E), accounting for the eastward advection of anomalies over time (Fig. 3).

It is difficult to continue to support an explanation for a circumpolar sea ice reduction that relies only on the confluence of regional atmospheric modes. While the spring 2016 sea ice decline has been attributed to anomalous atmospheric circulation^{17,20,30,32}, here we provide evidence supporting the hypothesis of Meehl et al.³⁰ that the warm subsurface ocean was an additional and important driver of the low sea ice in spring 2016 (Fig. 3c) and the sustained low sea ice state since.

Changed sea ice persistence. The characteristics of Antarctic sea ice persistence in the new low sea ice state have also changed, strengthening the suggestion of a regime shift in sea ice behaviour. However, there are considerable challenges in understanding these changes and the processes at play due to the limited length of the sea ice time series and the paucity of ocean observations from under the sea ice. Nevertheless, when taken in concert with the evidence presented above, these changed persistence characteristics provide further support that the subsurface ocean warming is linked with the current low sea ice state.

Prior to 2016, maximum sea ice coverage in austral spring (occurring from mid-September to early October) was correlated with minimum sea ice coverage in the following austral summer (occurring mid-February to early March; Fig. 4a; over 1979/80–2015/16, $r = 0.33$, $p < 0.05$, and over 2007/08–2015/16 $r = 0.62$, $p < 0.10$) – more sea ice coverage at the spring maximum was associated with more sea ice coverage at the summer minimum, and vice versa. This relationship can be understood in terms of persistence, via the ice-albedo and ocean heat uptake feedbacks, whereby higher sea ice coverage in spring increases the albedo and reduces solar ocean warming in subsequent months,

leading to a cooler surface ocean and higher sea ice coverage into summer^{2,33}. Spring sea ice anomalies have also been shown to influence subsequent autumn sea ice anomalies in a re-emergence process involving mixed layer feedbacks³⁴.

It is challenging to assess statistical changes in sea ice persistence during the recent period, given the small sample size ($N = 7$). Noting this limitation and treating results with caution, we find, since 2016, maximum sea ice coverage in spring is no longer correlated with minimum sea ice coverage in the following summer (Fig. 4a; over 2016/17–2021/23 $r = 0.27$, $p \sim 0.5$). Remarkably, in this recent period, minimum sea ice coverage in summer is found to be related with maximum sea ice coverage in the following spring (Fig. 4b; $r = 0.91$, $p < 0.01$), representing a fundamental change in the behaviour of Antarctic sea ice. Prior to 2016, there was not a relationship between minimum sea ice extent and the subsequent sea ice maximum (Fig. 4b; over 1979–2015 $r = 0.16$, $p \sim 0.3$), consistent with the previously identified predictability barrier in winter, whereby the upper ocean memory in the Winter Water layer linked with sea ice persistence is lost over mid-winter when Circumpolar Deep Water is entrained into the surface mixed layer³⁴. Since 2016, the link between sea ice at the minimum and the subsequent maximum eight months later suggests a central role for changed subsurface ocean conditions in the current sea ice regime. Observational studies are needed to understand the processes driving these changed sea ice persistence characteristics, highlighting the urgent need for oceanic observations under the sea ice. Process-based knowledge of the ocean-sea ice feedbacks can also be gained through modelling studies. This is beyond the scope of this contribution but will be the focus of a future study.

Multidecadal variability and change in the Southern Ocean.

Our change point analysis demonstrates that since 2016, Antarctic sea ice has been in a low-sea ice state, which is statistically distinguishable from the earlier part of the sea ice record (Fig. 1a). We present strong evidence that the subsurface ocean warming began prior to the 2016 change point (Figs. 1c, 3c) and has persisted since, and we suggest that this warm subsurface ocean is contributing to the current low sea ice state. The length of the sea ice record and the current period makes it difficult to determine whether this low sea ice state constitutes a regime shift in

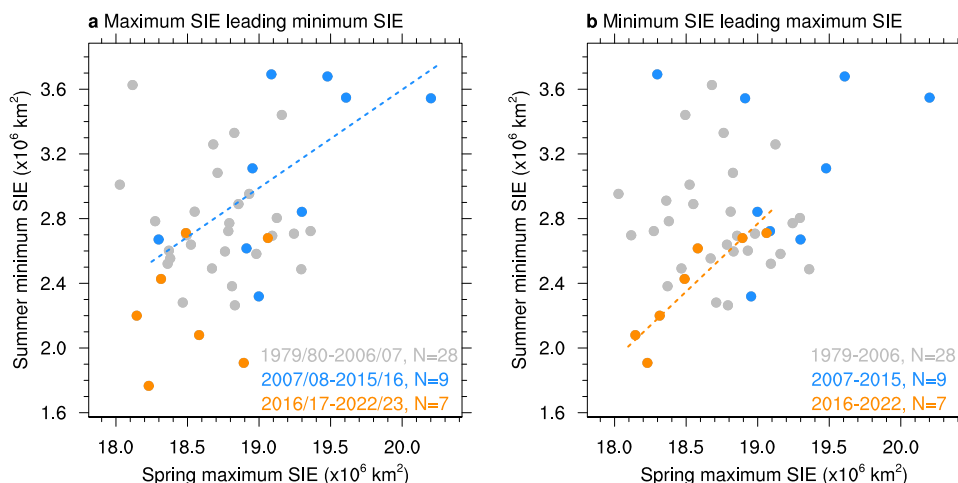


Fig. 4 Sea ice extent persistence characteristics have changed in the new low sea ice state. Relationships between **a** Spring (September–October) maximum sea ice extent (SIE) and the following summer (February–March) minimum SIE, and **(b)** minimum summer SIE and the following spring maximum SIE. Years in the first period (November 1978 to August 2007) are marked in grey, years in the second period (September 2007 to August 2016) are marked in blue, and years in the third period (September 2016 to May 2023) are marked in orange. In **(b)**, the change points occur between the summer minimum and spring maximum, and points are classified based on the spring maximum. In **(a)**, blue points are correlated (shown by the dashed blue line) with $r = 0.62$, $p < 0.10$. In **(b)**, orange points are correlated (shown by the dashed orange line) with $r = 0.91$, $p < 0.01$.

Antarctic sea ice^{22,26}, however we provide additional evidence supporting this. Namely, in the current low sea ice state, sea ice coverage is more tightly linked to the subsurface ocean conditions (Fig. 3), sea ice persistence characteristics have changed (Fig. 4), and the seasonal sea ice response to climate drivers has changed (e.g. the sea ice response to phases of the Southern Annular Mode, discussed above).

We cannot rule out the possibility that we are simply witnessing variability of the Antarctic sea ice system. There is large multidecadal variability in the Southern Ocean and Antarctic sea ice^{31,35,36}, and over the 44-year sea ice record our change point analysis identifies three different sea ice states (Fig. 1a). A continuation of the low sea ice state in years to come would provide further support for a new regime for Antarctic sea ice.

It is also unclear whether the observed ocean warming is the manifestation of the second long-term warming phase of the two-timescale response to prolonged strengthened westerly winds seen in coupled climate models – Ferreira et al.³⁷ proposed that the surface Southern Ocean response to strengthened westerly winds occurred over two distinct timescales: a rapid cooling due to enhanced northwards Ekman transport and vertical mixing, and a long-term warming due to upwelling of warmer subsurface waters. In this context, it is noteworthy that the current observed ocean warming follows a period of surface cooling³⁵, consistent with the first short-term cooling phase of the two-timescale response, and that both the initial cooling and subsequent near-surface ocean warming have occurred under a backdrop of prolonged Ekman upwelling (Supplementary Fig. 3). However, the mechanism behind the hypothesised long-term warming response³⁷ has been questioned³⁸, and there is a large spread across climate models in their transition time from rapid surface cooling to long-term surface warming^{39,40}. Regardless of whether the subsurface warming represents the second long-term warming phase of the two-timescale response or not, there is a clear signal of sustained subsurface warming that strengthens just prior to the beginning of the new low sea ice regime and persists until the present.

The role of Antarctic meltwater also remains uncertain and accelerated meltwater entering the Southern Ocean may yet counter the influences of increasing global temperatures on Antarctic sea ice coverage^{41–43}. Meltwater-induced surface freshening increases the near-surface stratification of the Southern Ocean, reducing convective overturning and the entrainment of warm subsurface waters into the surface layer, and thus results in a surface cooling conducive to increased sea ice coverage^{41,44}. However, the current low sea ice state is occurring at a time when Antarctic ice sheet and shelf melting is accelerating⁴⁵, and there are many uncertainties regarding the magnitude of the sea ice response to meltwater⁴⁶. The global climate implications of Antarctic meltwater are profound⁴⁷, and a concerted effort is needed to better understand meltwater impacts on sea ice over both the satellite era, and over the 21st Century^{44,46}.

Implications. The current extremely low sea ice will have a range of impacts. Changed ocean stratification and circulation will alter basal melting beneath ice shelves⁴⁸. Greater coastal exposure will increase coastal erosion and reduce ice-shelf stability⁴⁹. Changes in dense shelf water production will alter bottom water formation and deep ocean ventilation⁵⁰. Sea ice changes will also have contrasting influences on Adélie and emperor penguin colonies^{51,52}, and substantially alter human activities along the Antarctic coastline.

Anthropogenic greenhouse gas emissions have been attributed as the primary cause of Southern Ocean warming^{28,29}, and here

we suggest a potential link to a regime shift in Antarctic sea ice. While for many years, Antarctic sea ice increased despite increasing global temperatures⁶, it appears that we may now be seeing the inevitable decline, long projected by climate models⁵³. The far-reaching implications of Antarctic sea ice loss highlight the urgent need to reduce greenhouse gas emissions.

Methods

Sea ice extent data. We use the National Snow and Ice Data Center Southern Hemisphere version 3 daily, five-day and monthly sea ice extent indices⁴, which extend from November 1979 to June 2023. The daily sea ice extent index is used for the record daily extent cited in text, and we subtract the annual daily minimum averaged over 1979–2022 to calculate the daily minimum anomaly. The monthly sea ice extent index is used for record monthly extent, and for the time series analysis. We subtract the monthly climatology over 1979–2022 to produce monthly sea ice extent anomalies (Fig. 1a). December 1987 and January 1988 are missing from the sea ice extent index due to satellite retrieval issues in these months. We interpolate the monthly anomalies from November 1987 to February 1988 for these months, following Simmonds⁵⁴. Similarly, we subtract the five-day climatology averaged over 1979–2022 to produce five-day sea ice extent index anomalies time series, without any interpolation in 1987/88 in this case (Fig. 2).

The absolute magnitude of sea ice extent anomalies during the late summer months is limited by the climatologically low sea ice coverage at this time. To better examine the anomalous sea ice coverage occurring during the summer minimum months, we express the sea ice extent anomalies as a percentage of the 1979–2022 monthly climatology. This method reveals exceptional sea ice minima in the post-2016 period (Fig. 1b).

Change point analysis. We apply an algorithm to the sea ice extent anomaly time series (Fig. 1a) to detect change points in the mean, with the optimal fit found minimising Bayesian information criterion and allowing for multiple change points, using R package *changepoint*⁵⁵ (with penalty = BIC, method = PELT). Bayesian information criteria is a measure of model fit using log-likelihood, the model complexity and number of observations, and is used to assess relative model performance⁵⁶. The model with the lowest Bayesian information criteria thus provides the best model fit using the least number of model parameters. The advantage of using Bayesian information criteria is that by penalising complex models it excludes short periods of smaller fluctuations allowing identification of the most significantly different periods. Two change points are identified over the 44-year time series, August 2007 and August 2016 (the last months in each segment), separating the sea ice anomaly record into three periods with statistically distinguishable means.

This process is repeated to detect change points in linear regression models of the time series, again with the optimal fit found by minimising the Bayesian information criterion and allowing for multiple change points, using the R package *strucchange*⁵⁷ (with optimal model = BIC, $h = 0.15$, where h is the default cut-off length as a fraction of time series length). Three change points are identified using this method, August 1993, November 2007 and August 2016, separating the sea ice anomaly record into four periods. When forced to detect only two change points, this algorithm identifies August 2007 and August 2016 as change points. This algorithm is not detecting changes in the mean of different periods, but rather changes in the linear fit of different periods. While an additional change point is detected using *strucchange* (August 1993), the second and third change points detected using *strucchange* are very similar to those found

using *changeoint*, demonstrating the robustness of the winter/spring 2007 and August 2016 change points across detection methods. We therefore focus on the two later change points in our analysis.

We compare the variance and mean of the three periods using F-tests and t-tests, respectively. As described in the main text, this shows variability in the first period is lower than in the subsequent periods (F-test, $p < 0.01$), but variability in the two later periods is not statistically distinguishable. Taking this into account, the t-tests to compare the mean of the first period with the means of the two later periods assumes different population variances (Welsh's t-test), while the t-test to compare the means of the two later periods assumes the samples have the same population variance.

Large-scale climate modes. Large-scale climate drivers can influence Antarctic sea ice variability^{7,8,10}. To examine the possible contribution of climate drivers to the shift in Antarctic sea ice extent to its current low state, monthly time series are obtained for the Southern Annular Mode, the Southern Oscillation Index, the Interdecadal Pacific Oscillation, the Indian Ocean Dipole, and the Atlantic Multidecadal Oscillation. All monthly indices are smoothed with a rolling mean using a two-year centred window. Values within half a standard deviation of zero are masked, and the sign of each index is extracted and examined. The identified sea ice anomaly change points do not align with sign changes in any of the climate indices (Supplementary Fig. 1).

Ocean temperature data. Ocean temperature data from January 2004 to May 2023 are derived from the extension of the gridded Argo data product described in ref. ⁵⁸. This product is a $1^\circ \times 1^\circ$ gridded atlas of monthly mean profiles for ocean temperature and salinity from the surface to 2000 dBar, based on data from Argo profiling floats. While this dataset does not include shipboard measurements, it provides broad spatial coverage of the Southern Ocean within a homogenous dataset. This allows us to take large-scale spatial means without biasing the results towards particular regions. The number of floats in the global Argo array increased following initial deployments and reached 3000 floats in 2007. Correspondingly, the density of measurements in the first years of the Argo dataset is lower than in later years. As such, the first few years of the gridded data product are likely to be overly influenced by the long-term climatology used as an initial guess in the gridding process. Historically, Argo floats suffered from high mortality rates in sea ice covered regions. The implementation of sea ice avoidance algorithms and hardware changes has improved the durability of Argo floats operating in seasonally ice-covered regions. However, the paucity of data in these regions means that the gridded data product we use is limited to regions north of the seasonal sea ice zone in the Southern Ocean. As such, the temperature anomalies that we plot are from north of the sea ice extent anomalies.

The 2004–2022 monthly climatology is subtracted from the dataset to produce monthly mean temperature anomalies. The depth-time temperature anomaly was calculated as a circumpolar average between $50\text{--}65^\circ\text{S}$, following Meehl et al.³⁰. We obtain very similar results when the circumpolar average is calculated over $55\text{--}65^\circ\text{S}$ (not shown). Grid aware averages were calculated using the *xgcm* Python package⁵⁹. Temperature anomalies are converted to depth levels for plotting (Fig. 1c).

We assess the magnitude of the zonal-mean ocean temperature anomalies relative to the variance (± 1 standard deviation) but note that this is not a strong indication of statistical significance. Because of the large underlying trend in ocean anomalies over the Argo period, the variance of the temperature anomalies is

inflated, and very few of the anomalies exceed the ± 2 standard deviation envelope when calculated on depth levels. We perform a linear regression on the temperature anomalies at each depth level and find the linear trend to be statistically significant at all depth levels ($p < 2.5e^{-6}$), with a magnitude of $0.09^\circ\text{C decade}^{-1}$ near the surface and $0.03^\circ\text{C decade}^{-1}$ at 500 m (Supplementary Fig. 4).

Sea ice concentration data. Spatial patterns in anomalous longitudinal sea ice extent and sea ice concentration are also assessed (Fig. 3 and Supplementary Fig. 2). We use the National Snow and Ice Data Center Southern Hemisphere version 4 Climate Data Record monthly sea ice concentration, which extends from November 1978 to May 2023. January to May 2023 are near real time interim data, version 2. Longitudinal sea ice extent is calculated using sea ice concentration regridded to a $1^\circ \times 1^\circ$ grid. For each longitude, the area of grid cells where sea ice concentration is greater than 15% is summed to give the longitudinal sea ice extent. We subtract the monthly climatology averaged over 1979–2022 to calculate the monthly anomalies.

Hovmöller analysis. The temporal evolution of longitudinal sea ice extent and ocean temperature averaged over $50\text{--}65^\circ\text{S}$ and two depth intervals, 0–100 m and 100–200 m, is depicted in Hovmöller diagrams (Fig. 3). Smoothing is applied to the sea ice extent and temperature fields using a running average both temporally (over 12 months) and longitudinally (over 20°).

Composite analysis. Spatial patterns in anomalous sea ice concentration (relative to the 1979–2022 climatology) and ocean temperature (100–200 m; relative to the 2004–2022 climatology) are also assessed (Supplementary Fig. 2). Statistical significance of the sea ice concentration and ocean temperature changes are assessed using Welch's unequal variance t-test at each grid point in the Southern Ocean. We assess the significance of the sea ice concentration anomalies in the second and third periods with respect to the sea ice concentration over the full duration of the first period, November 1978 to August 2007. Ocean temperature data from January 2004 to August 2007 is compared with data from each of the subsequent periods. A Bonferroni correction is applied to avoid false positives (Type 1 error); the corrected p-value for statistical significance becomes $0.05/15/360 \sim 9e^{-6}$. This represents a highly conservative estimate for statistical significance since the grid points are not entirely independent and the Bonferroni correction is intrinsically conservative.

Surface wind stress and Ekman pumping. We use monthly surface eastward and northward turbulent wind stresses from the fifth generation European Centre for Medium-Range Weather Forecasts atmospheric reanalysis⁶⁰, annually averaged over both the Argo period 2004–2022 and the satellite period 1979–2022, to calculate downward Ekman pumping (Supplementary Fig. 3). Ekman pumping, w_E , is calculated as $w_E = (\nabla \times \boldsymbol{\tau}/f)/\rho$, where $\nabla \times \boldsymbol{\tau}$ is the surface wind stress curl, f is the Coriolis parameter and ρ is the density of seawater, approximated here as 1025 kg m^{-3} .

Data availability

Data related to the paper can be downloaded from the following:

- National Snow and Ice Data Center sea ice extent: <https://nsidc.org/data/g02135/versions/3>
- National Snow and Ice Data Center Climate Data Record version 4 and Near Real Time version 2 of sea ice concentration: <https://nsidc.org/data/g02202/versions/4> and <https://nsidc.org/data/g10016/versions/2>
- Argo ocean temperature data: https://sio-argo.ucsd.edu/RG_Climatology.html

- European Centre for Medium-Range Weather Forecasts fifth generation atmospheric reanalysis: <https://cds.climate.copernicus.eu/cdsapp#!/dataset/reanalysis-era5-complete?tab=overview>
- Southern Annular Mode: <http://www.nerc-bas.ac.uk/icd/gjma/sam.html>
- Interdecadal Pacific Oscillation: <https://psl.noaa.gov/data/timeseries/IPOTPI/>
- Southern Oscillation Index: <https://www.ncdc.noaa.gov/access/monitoring/enso/soi>
- Atlantic Multidecadal Oscillation: <https://psl.noaa.gov/data/timeseries/AMO>
- Indian Ocean Dipole: <https://stateoftheocean.osmc.noaa.gov/sur/ind/dmi.php>

Code availability

Analysis code to reproduce the change point detection, Figs. 1–4 and Supplementary Figs. 2, 3 are available at <https://github.com/ariaanp/2023-sea-ice-regime>. Analysis code to reproduce the ocean temperature time-series and Supplementary Figs. 1 and 4 are available at <https://github.com/edoddridge/2023-sea-ice-regime>.

Received: 5 July 2023; Accepted: 14 August 2023;

Published online: 13 September 2023

References

- Meehl, G. A. Modeling the Earth's climate. *Clim. Change* **6**, 259–286 (1984).
- Stammerjohn, S., Massom, R. A., Rind, D. & Martinson, D. G. Regions of rapid sea ice change: an inter-hemispheric seasonal comparison. *Geophys. Res. Lett.* **39**, L06501 (2012).
- Rintoul, S. R. The global influence of localized dynamics in the Southern Ocean. *Nature* **558**, 209–218 (2018).
- Fetterer, F., Knowles, K., Meier, W.N., Savoie, M. & Windnagel, A.K. Sea Ice Index, Version 3 [Data Set]. Boulder, Colorado USA. National Snow and Ice Data Center. [Date Accessed 04-02-2023] <https://doi.org/10.7265/N5K072F8> (2017).
- Raphael, M. N. & Handcock, M. S. A new record minimum for Antarctic sea ice. *Nat. Rev. Earth Environ.* **3**, 215–216 (2022).
- Parkinson, C. L. A 40-y record reveals gradual Antarctic sea ice increases followed by decreases at rates far exceeding the rates seen in the Arctic. *Proc. Natl. Acad. Sci. USA* **116**, 14414–14423 (2019).
- Doddridge, E. W. & Marshall, J. Modulation of the Seasonal Cycle of Antarctic Sea Ice Extent Related to the Southern Annular Mode. *Geophys. Res. Lett.* **44**, 9761–9768 (2017).
- Purich, A. et al. Tropical Pacific SST Drivers of Recent Antarctic Sea Ice Trends. *J. Clim.* **29**, 8931–8948 (2016).
- Meehl, G. A., Arblaster, J. M., Bitz, C. M., Chung, C. T. Y. & Teng, H. Antarctic sea-ice expansion between 2000 and 2014 driven by tropical Pacific decadal climate variability. *Nat. Geosci.* **9**, 590–595 (2016).
- Simpkins, G. R., McGregor, S., Taschetto, A. S., Ciasto, L. M. & England, M. H. Tropical Connections to Climatic Change in the Extratropical Southern Hemisphere: The Role of Atlantic SST Trends. *J. Clim.* **27**, 4923–4936 (2014).
- Li, X., Holland, D. M., Gerber, E. P. & Yoo, C. Impacts of the north and tropical Atlantic Ocean on the Antarctic Peninsula and sea ice. *Nature* **505**, 538–542 (2014).
- Holland, P. R. & Kwok, R. Wind-driven trends in Antarctic sea-ice drift. *Nat. Geosci.* **5**, 872–875 (2012).
- Purich, A., Cai, W., England, M. H. & Cowan, T. Evidence for link between modelled trends in Antarctic sea ice and underestimated westerly wind changes. *Nat. Commun.* **7**, 10409 (2016).
- Bintanja, R., van Oldenborgh, G. J., Drijfhout, S. S., Wouters, B. & Katsman, C. A. Important role for ocean warming and increased ice-shelf melt in Antarctic sea-ice expansion. *Nat. Geosci.* **6**, 376–379 (2013).
- Pauling, A. G., Smith, I. J., Langhorne, P. J. & Bitz, C. M. Time-Dependent Freshwater Input From Ice Shelves: Impacts on Antarctic Sea Ice and the Southern Ocean in an Earth System Model. *Geophys. Res. Lett.* **44**, 454–410,461 (2017).
- Lecomte, O. et al. Vertical ocean heat redistribution sustaining sea-ice concentration trends in the Ross Sea. *Nat. Commun.* **8**, 258 (2017).
- Schlosser, E., Haumann, F. A. & Raphael, M. N. Atmospheric influences on the anomalous 2016 Antarctic sea ice decay. *Cryosphere* **12**, 1103–1119 (2018).
- Turner, J. et al. Record Low Antarctic Sea Ice Cover in February 2022. *Geophys. Res. Lett.* **49**, e2022GL098904 (2022).
- Yadav, J., Kumar, A. & Mohan, R. Atmospheric precursors to the Antarctic sea ice record low in February 2022. *Environ. Res. Commun.* **4**, 121005 (2022).
- Turner, J. et al. Unprecedented springtime retreat of Antarctic sea ice in 2016. *Geophys. Res. Lett.* **44**, 6868–6875 (2017).
- Marshall, G. J. Trends in the Southern Annular Mode from observations and reanalyses. *J. Clim.* **16**, 4134–4143 (2003).
- Schroeter, S., O'Kane, T. J. & Sandery, P. A. Antarctic sea ice regime shift associated with decreasing zonal symmetry in the Southern Annular Mode. *Cryosphere* **17**, 701–717 (2023).
- Gille, S. T. Warming of the Southern Ocean Since the 1950s. *Science* **295**, 1275–1277 (2002).
- Armour, K. C., Marshall, J., Scott, J. R., Donohoe, A. & Newsom, E. R. Southern Ocean warming delayed by circumpolar upwelling and equatorward transport. *Nat. Geosci.* **9**, 549–554 (2016).
- Shi, J.-R., Talley, L. D., Xie, S.-P., Peng, Q. & Liu, W. Ocean warming and accelerating Southern Ocean zonal flow. *Nat. Clim. Change* **11**, 1090–1097 (2021).
- Eayrs, C., Li, X., Raphael, M. N. & Holland, D. M. Rapid decline in Antarctic sea ice in recent years hints at future change. *Nat. Geosci.* **14**, 460–464 (2021).
- Solomon, A., Polvani, L. M., Smith, K. L. & Abernathy, R. P. The impact of ozone depleting substances on the circulation, temperature, and salinity of the Southern Ocean: An attribution study with CESM1(WACCM). *Geophys. Res. Lett.* **42**, 5547–5555 (2015).
- Swart, N. C., Gille, S. T., Fyfe, J. C. & Gillett, N. P. Recent Southern Ocean warming and freshening driven by greenhouse gas emissions and ozone depletion. *Nat. Geosci.* **11**, 836–841 (2018).
- Hobbs, W. R., Roach, C., Roy, T., Sallée, J.-B. & Bindoff, N. Anthropogenic Temperature and Salinity Changes in the Southern Ocean. *J. Clim.* **34**, 215–228 (2021).
- Meehl, G. A. et al. Sustained ocean changes contributed to sudden Antarctic sea ice retreat in late 2016. *Nat. Commun.* **10**, 14 (2019).
- Rathore, S., Bindoff, N. L., Phillips, H. E. & Feng, M. Recent hemispheric asymmetry in global ocean warming induced by climate change and internal variability. *Nat. Commun.* **11**, 2008 (2020).
- Wang, G. et al. Compounding tropical and stratospheric forcing of the record low Antarctic sea-ice in 2016. *Nat. Commun.* **10**, 13 (2019).
- Holland, P. R. The seasonality of Antarctic sea ice trends. *Geophys. Res. Lett.* **41**, 4230–4237 (2014).
- Libera, S., Hobbs, W., Klocker, A., Meyer, A. & Matear, R. Ocean-Sea Ice Processes and Their Role in Multi-Month Predictability of Antarctic Sea Ice. *Geophys. Res. Letters* **49**, e2021GL097047–e092021GL097047 (2022).
- Fan, T., Deser, C. & Schneider, D. P. Recent Antarctic sea ice trends in the context of Southern Ocean surface climate variations since 1950. *Geophys. Res. Lett.* **41**, 2419–2426 (2014).
- Fogt, R. L., Sleinkofer, A. M., Raphael, M. N. & Handcock, M. S. A regime shift in seasonal total Antarctic sea ice extent in the twentieth century. *Nat. Clim. Change* **12**, 54–62 (2022).
- Ferreira, D., Marshall, J., Bitz, C. M., Solomon, S. & Plumb, A. Antarctic Ocean and Sea Ice Response to Ozone Depletion: A Two-Time-Scale Problem. *J. Clim.* **28**, 1206–1226 (2015).
- Doddridge, E. W. et al. Eddy Compensation Dampens Southern Ocean Sea Surface Temperature Response to Westerly Wind Trends. *Geophys. Res. Lett.* **46**, 4365–4377 (2019).
- Kostov, Y. et al. Fast and slow responses of Southern Ocean sea surface temperature to SAM in coupled climate models. *Clim. Dyn.* **48**, 1595–1609 (2016).
- Seviour, W. J. M. et al. The Southern Ocean Sea Surface Temperature Response to Ozone Depletion: A Multimodel Comparison. *J. Clim.* **32**, 5107–5121 (2019).
- Bronslaer, B. et al. Change in future climate due to Antarctic meltwater. *Nature* **564**, 53–58 (2018).
- Golledge, N. R. et al. Global environmental consequences of twenty-first-century ice-sheet melt. *Nature* **566**, 65–72 (2019).
- Sadai, S., Condrón, A., DeConto, R. & Pollard, D. Future climate response to Antarctic Ice Sheet melt caused by anthropogenic warming. *Sci. Adv.* **6** <https://doi.org/10.1126/sciadv.aaz1169> (2020).
- Purich, A. & England, M. H. Projected Impacts of Antarctic Meltwater Anomalies over the Twenty-First Century. *J. Clim.* **36**, 2703–2719 (2023).
- Greene, C. A., Gardner, A. S., Schlegel, N.-J. & Fraser, A. D. Antarctic calving loss rivals ice-shelf thinning. *Nature* **609**, 948–953 (2022).
- Swart, N. et al. The Southern Ocean Freshwater release model experiments Initiative (SOFIA): Scientific objectives and experimental design. *EGU Sphere* **2023**, 1–30 (2023).
- Li, Q., England, M. H., Hogg, A. M., Rintoul, S. R. & Morrison, A. K. Abyssal ocean overturning slowdown and warming driven by Antarctic meltwater. *Nature* **615**, 841–847 (2023).
- Aoki, S. et al. Warm surface waters increase Antarctic ice shelf melt and delay dense water formation. *Commun. Earth Environ.* **3**, 142–142 (2022).
- Reid, P. A. & Massom, R. A. Change and variability in Antarctic coastal exposure, 1979–2020. *Nat. Commun.* **13**, 1164–1164 (2022).
- Silvano, A. et al. Recent recovery of Antarctic Bottom Water formation in the Ross Sea driven by climate anomalies. *Nat. Geosci.* **13**, 780–786 (2020).

51. Watanabe, Y. Y., Ito, K., Kokubun, N. & Takahashi, A. Foraging behavior links sea ice to breeding success in Antarctic penguins. *Sci. Adv.* **6**, eaba4828–eaba4828 (2023).
52. Fretwell, P. T. & Trathan, P. N. Emperors on thin ice: three years of breeding failure at Halley Bay. *Antarctic Sci.* **31**, 133–138 (2019).
53. Fox-Kemper, B., et al. Ocean, Cryosphere and Sea Level Change. In *Climate Change 2021: The Physical Science Basis. Contribution of Working Group I to the Sixth Assessment Report of the Intergovernmental Panel on Climate Change* [Masson-Delmotte, et al. (eds.)]. Cambridge University Press, Cambridge, United Kingdom and New York, NY, USA, 1211–1362. (2021).
54. Simmonds, I. Comparing and contrasting the behaviour of Arctic and Antarctic sea ice over the 35 year period 1979–2013. *Ann. Glaciol.* **56**, 18–28 (2015).
55. Killick R., Haynes K., & Eckley, I.A. changepoint: An R package for changepoint analysis. R package version 2.2.4. <https://CRAN.R-project.org/package=changepoint> (2022).
56. Schwarz, G. Estimating the Dimension of a Model. *Ann. Stat.* **6**, 461–464 (1978).
57. Zeileis, A., Leisch, F., Hornik, K. & Kleiber, C. strucchange: an R package for testing for structural change in linear regression models. *J. Stat. Softw.* **7**, 1–38 (2002).
58. Roemmich, D. & Gilson, J. The 2004–2008 mean and annual cycle of temperature, salinity, and steric height in the global ocean from the Argo Program. *Prog. Oceanogr.* **82**, 81–100 (2009).
59. Abernathey, R.P., et al. Xgcm (v0.8.1). Zenodo, <https://doi.org/10.5281/ZENODO.7348619> (2022).
60. Hersbach, H. et al. The ERA5 global reanalysis. *Quart. J. Royal Meteorol. Soc.* **146**, 1999–2049 (2020).

Acknowledgements

A.P. and E.W.D. are recipients of an Australian Research Council Discovery Project (DP230102994) funded by the Australian Government. This work was supported by the Australian Research Council Special Research Initiative for Securing Antarctica's Environmental Future (SR200100005). This project received grant funding from the Australian Government as part of the Antarctic Science Collaboration Initiative program (ASCI000002). We thank Julie Arblaster for insightful discussions and Vaughn Grey for assistance with the change point detection. We also thank Zach Labe for his Antarctic sea ice visualisations shared on Twitter (@ZLabe) that inspired Fig. 2. We thank four anonymous reviewers for insightful comments.

Author contributions

A.P. and E.W.D. conceived the study, wrote the initial manuscript, conducted the analysis, reviewed, edited and improved the paper.

Competing interests

The authors declare no competing interests.

Additional information

Supplementary information The online version contains supplementary material available at <https://doi.org/10.1038/s43247-023-00961-9>.

Correspondence and requests for materials should be addressed to Ariaan Purich.

Peer review information *Communications earth and environment* thanks the anonymous reviewers for their contribution to the peer review of this work. Primary Handling Editors: Heike Langenberg. A peer review file is available.

Reprints and permission information is available at <http://www.nature.com/reprints>

Publisher's note Springer Nature remains neutral with regard to jurisdictional claims in published maps and institutional affiliations.



Open Access This article is licensed under a Creative Commons Attribution 4.0 International License, which permits use, sharing, adaptation, distribution and reproduction in any medium or format, as long as you give appropriate credit to the original author(s) and the source, provide a link to the Creative Commons licence, and indicate if changes were made. The images or other third party material in this article are included in the article's Creative Commons licence, unless indicated otherwise in a credit line to the material. If material is not included in the article's Creative Commons licence and your intended use is not permitted by statutory regulation or exceeds the permitted use, you will need to obtain permission directly from the copyright holder. To view a copy of this licence, visit <http://creativecommons.org/licenses/by/4.0/>.

© The Author(s) 2023